

Analysis of the normal-state resistivity for the neutron-irradiated *A15* superconductors V_3Si , Nb_3Pt , and Nb_3Al

R. Caton*

Brookhaven National Laboratory, Upton, New York 11973

R. Viswanathan

Hughes Aircraft Company, Culver City, California 90230

(Received 7 April 1981; revised manuscript received 11 August 1981)

The normal-state resistivity of the *A15* superconductors V_3Si , Nb_3Pt , and Nb_3Al has been studied as a function of neutron damage. Resistivity data have been taken from the superconducting transition temperature T_c to room temperature on unirradiated samples and irradiated samples with degraded T_c 's ranging down to 2–3 K. The V_3Si data are the most extensive and both a single-crystal and polycrystalline samples have been studied. The Nb_3Pt and Nb_3Al data were taken for comparison. The data are fitted to several theoretical expressions put forth to explain the normal-state resistivity in *A15* superconductors at low temperatures, high temperatures, and the full range of temperatures. The results are discussed in light of these theories. The most striking feature of the V_3Si data is that there is no observable change in the shape of the temperature-dependent contribution to the resistivity down to a fractional degradation of T_c of ~ 0.5 . This does not appear to be the case for the Nb-based *A15* superconductors. It is suggested that this difference in behavior may be related to the different sensitivity of T_c to disorder in V_3Si as opposed to the Nb-based *A15* superconductors.

I. INTRODUCTION

The normal-state resistivity of high-transition-temperature (T_c) superconductors has been of considerable interest for several years. This interest has grown in the recent years and attempts have been made to understand the rather distinctive temperature (T) dependence of the resistivity (ρ) and relate it to T_c (e.g., see Refs. 1–9). One of the most striking features in the resistivity data common to many high- T_c superconductors is a strong saturation of ρ at high T rather than the linear dependence predicted by the classical Bloch-Grüneisen theory.¹⁰ This behavior has been reported in many high- T_c superconductors: several cubic structures,¹ *A15* compounds,^{11,12} Laves phases,¹³ and most recently the Chevrel phases.¹⁴ It should be noted that the saturation behavior is seen in nonsuperconducting elements¹⁵ also and not in all high- T_c superconductors.¹ However, the near ubiquity of this feature in high- T_c superconductors is enough incentive to stimulate further studies. We undertook an investigation of the effect of neutron irradiation on the resistivity of *A15* compounds which concentrated mostly on V_3Si with some data on Nb_3Al and Nb_3Pt for comparison. Through neutron damage, it is possible to lower the T_c (Ref. 16) and thus systematically analyze the relation between resistivity (magnitude and temperature dependence) and T_c for a single system. This avoids the inherent difficulties in comparing data on different samples

prepared in different manners. Studies of the effects of electron irradiation (Nb_3Sn and Nb_3Ge),¹⁷ α -particle irradiation (several *A15*'s),^{6,18,19} and neutron irradiation (Nb_3Sn and V_3Si)^{20,21} on the electrical resistivity have been reported by other investigators.

As the purpose of this work is to follow the relation between resistivity and T_c , we have analyzed our data in terms of several theories proposed to describe the resistivity in *A15* compounds. Woodard and Cody²² were the first to attack this problem by fitting Nb_3Sn data to the empirical formula

$$\rho = \rho_0 + \rho_1 T + C e^{-T_0/T}, \quad (1)$$

where ρ_0 is the residual resistivity and ρ_1 , c , and T_0 are all constants. The second and third terms represent the high- and low-temperature limits of the occupation number of a particular phonon which assists in interband scattering according to Wilson's model of *s-d* scattering. Unfortunately, the ratio C/ρ_1 from the Nb_3Sn data is not consistent with Wilson's theory.²² More recently, Milewits, Williamson, and Taub²³ have suggested the modification

$$\rho = \rho_0 + \rho_1 T^n + C e^{-T_0/T}, \quad (2)$$

where they suggest that the third term arises from phonon-assisted scattering between two pockets of the Fermi surface. But rather than interpret the second term according to Woodard and Cody as the high-temperature limit of the Wilson theory, they propose the second term to express a separate low-

temperature contribution to the resistivity and allow the exponent n to vary. They find an exponent $n = \frac{3}{2}$ or 2 best fits their data on V_3Si .

Cohen, Cody, and Halloran²⁴ (RCA model) were able to fit the saturation of ρ in the Nb_3Sn data by assuming the existence of sharp structure in the density of states near the Fermi level E_F (in fact, they chose a step function). A sharp structure in the density of states is reasonable for $A15$'s where there is a high-density-of-states d band overlying a low-density-of-states s band. Bader and Fradin⁵ have carried this further and shown that a more realistic smoothed electronic density of states (using half of a Gaussian function) also can explain the saturation seen in many high- T_c $A15$ compounds. Further, they show that a parabolic-model density of states can be used to describe the saturation observed in the low- T_c $A15$ Nb_3Sb . In other words, the existence of fine structure in the density of states near E_F can explain the observed saturation in resistivity.

Along other lines, Fisk and Webb³ suggest that the observed saturation in resistivity takes place when the mean free path is on the order of the interatomic spacing. At this point, the mean free path saturates and no longer depends linearly on the scattering perturbation. Thus the linear T dependence of ρ breaks down and the subsequent increase in ρ is less than linear. They point to data for pure Nb which indicates that the mean free path will be the order of the interatomic spacing when $\rho \approx 200 \mu\Omega \text{ cm}$ and this is the order of magnitude of saturation resistivities observed in $A15$'s. Recently, Allen *et al.*²⁵ have calculated "extremely short phonon-limited mean free paths" for the $A15$ compounds Nb_3Ge and Nb_3Al near room temperature which lends further support to the above idea. Wiesmann *et al.*⁶ have cast the idea of saturation and a maximum resistance into the empirical formula

$$\frac{1}{\rho} = \frac{1}{\rho_{\max}} + \frac{1}{\rho_{\text{ideal}}}, \quad (3)$$

where the ideal resistivity ρ_{ideal} , which can be characterized many ways, is "in parallel" with the saturation resistivity ρ_{\max} . One can separate ρ_{ideal} into two parts by writing $\rho_{\text{ideal}} = \rho_{0I}(T) + \rho_I(T)$, where ρ_{0I} is the ideal temperature-independent residual resistivity without the additional saturation channel and $\rho_I(T)$ is the corresponding ideal temperature dependent part. For higher-temperature data ($T \geq 200 \text{ K}$) one can characterize $\rho_I(T)$ by the limit of the Bloch-Grüneisen expression at high temperature or $\rho_I(T) = LT$, where L is a constant which is proportional to the strength of the electron-phonon coupling. For lower T one can try either Wilson's model of s - d scattering for transition metals

$$\rho_I(T) = \rho_{sd} = \kappa_{sd} \left(\frac{T}{\Theta_{sd}} \right)^3 \int_0^{\Theta_{sd}/T} \frac{x^3 dx}{(e^x - 1)(1 - e^{-x})}, \quad (4)$$

where Θ_{sd} is a cutoff similar to the Debye temperature and κ_{sd} is a constant or the Bloch-Grüneisen expression

$$\rho_I(T) = \rho_{\text{Grün}} = \kappa_R \frac{4T^5}{\Theta_R^6} \int_0^{\Theta_R/T} \frac{x^5 dx}{(e^x - 1)(1 - e^{-x})}, \quad (5)$$

where Θ_R is a cutoff, again similar to the Debye temperature, and κ_R is a constant. Recently, Chakraborty and Allen⁹ have generalized Boltzmann transport theory by including interband scattering and renormalization effects which become important at short mean free paths. This opens up a channel "reminiscent of hopping mechanisms" which accounts for Eq. (3).

Morton, James, and Wostenholm⁷ have obtained the form of Eq. (3) by modifying the Bloch-Mott-Wilson theory for transition metals. They include an efficiency factor which accounts for the reduced rate of scattering of the d electrons by phonons as the mean free path of the d electrons becomes the order of the interatomic spacing. Their expression for $\rho_I(T)$ is

$$\rho_I(T) = b_{sd} (T/\Theta_m)^r \int_0^{\Theta_m/T} \frac{x^r dx}{(e^x - 1)(1 - e^{-x})}, \quad (6)$$

where Θ_m is yet another cutoff temperature with b_{sd} the associated constant. This amounts to a generalization of the Wilson theory ($r=3$) or Bloch-Grüneisen model ($r=5$) for the ideal part of the resistivity.

Starting from extensions of Ziman's theory²⁶ of liquid metals, Cote and Meisel⁸ obtain the saturation effects observed in the resistivity of $A15$ compounds at high temperatures by incorporating the interaction postulate (attributed to Pippard) which can be stated as: "phonons whose wavelength exceeds the electron mean free path are ineffective electron scatterers." And, in a later paper,²⁷ they obtain a computed curve for a normalized T_c versus a normalized residual resistivity which saturates at low ρ_0 (i.e., below $\rho_0 \sim 40 \mu\Omega \text{ cm}$ T_c no longer increases but is constant). This result agrees well with data on α -particle damaged Nb_3Sn .²⁷

The $A15$ structure has a very striking feature in that there exists three mutually perpendicular chains of atoms and the atoms are more closely spaced within the chains than in any other direction. Gor'kov²⁸ assumes that to a first approximation the d electrons are localized on these chains and he locates the Fermi level at a high-symmetry point in reciprocal space. This leads to an instability of the electron spectrum at this point against electron-lattice and electron-electron interactions which leads to a structural transition ($\sim 50 \text{ K}$ in Nb_3Sn and $\sim 20 \text{ K}$ in V_3Si) in $A15$ compounds in agreement with observation. Above this transition Gor'kov's theory predicts a logarithmic temperature dependence for all quantities. In particular, the resistivity at high temperatures

can be expressed as

$$\rho = \rho_0 + A \ln(T/B) , \quad (7)$$

where ρ_0 is the usual constant residual resistivity and A and B are constants.

In addition to the interest in understanding the saturation of ρ at high T , there have also been attempts to explain the resistivity behavior at low T (from T_c to ~ 50 K or less). Marchenko²⁹ noted a T^2 dependence of the resistivity in V_3Si in the region $T_c \leq T \leq 29$ K. He attributed this to intraband electron-electron scattering and states that the ratio of b in the formula

$$\rho = \rho_0 + bT^2 \quad (8)$$

to γ^2 (γ is the electronic specific-heat coefficient) is comparable to ratios for transition metals where electron-electron scattering is assumed to predominate.³⁰ Unfortunately, the value of γ he used was per gram mole and if you use the value per gram atom as should be the case then there is a discrepancy of a factor of 16. The quantity b/γ^2 is really 16 times smaller than for the transition elements as pointed out by Webb *et al.*¹² for other $A15$'s. In fact, they show that the resistivity of Nb_3Sn between 20 and 50 K can be fit using the actual phonon density of states (rather than the Debye spectrum) assuming only phonon-assisted s - d interband scattering. It should be noted that the dependence in this case fits the T^2 data but they suggest this is only an accident due to the particular form for the actual phonon density of states. Bader and Fradin⁵ make a similar observation for V_3Si . Thus in these two cases it is the non-Debye character of the phonon spectrum which explains the ρ vs T data at low T .

Since we plan to follow these ideas concerning the nature of the resistivity in $A15$ compounds as a function of neutron damage, it would be appropriate at this point to interject a few very brief comments concerning the nature of radiation damage in $A15$ superconductors. Sweedler, Cox, and Moehlecke¹⁶ obtained a strong correlation between T_c and site-exchange disorder as T_c is degraded by neutron damage. Thus, they propose anti-site defects as the culprit in lowering T_c . From channeling experiments on α -irradiated V_3Si single crystals, Testardi *et al.*³¹ show that the results can be interpreted in terms of static displacement of the V atoms from their lattice sites. Perhaps both these defects are important in understanding radiation damage in $A15$ superconductors. However, Pande³² has pointed out that there is some question as to the uniformity of neutron-irradiated $A15$ superconductors and that it is necessary to consider the effect of inhomogeneity when discussing radiation damage in these compounds. In neutron-irradiated $A15$'s inhomogeneous regions on the scale of 40 Å have been observed.³² However, all

our present analysis assumes homogeneous damage; the effect of inhomogeneity on resistivity is not discussed here.

II. EXPERIMENT

A. Sample preparation

The $A15$'s studied in this work were V_3Si , Nb_3Al , and Nb_3Pt . The V_3Si single crystal was from a boule grown by Greiner and Mason³³ using a floating-zone melting technique and was adjacent to the large single crystal for which heat-capacity,³⁴ sound-velocity,³⁵ magnetic-susceptibility,³⁵ and neutron-scattering³⁶ measurements have been reported. The polycrystalline V_3Si samples were arc melted starting with Materials Research Corporation marz grade (99.9+%-pure) vanadium and semiconductor grade Si. The resulting samples were nominally $V_{75.1}Si_{24.9}$ as determined from weight-loss measurements. Before cutting and polishing flat the resistivity specimens, the V_3Si ingot was annealed at 800 °C for ~ 2 weeks. The Nb_3Al was prepared by Moehlecke³⁷ in a manner similar to the V_3Si except that the relatively high volatility of the aluminum made it much more difficult to prepare. The starting materials were spectroscopically pure Johnson Matthey Nb and 99.9%-pure Al from ROC/RIC. the nominal composition of the specimen we studied was $Nb_{75.5}Al_{24.5}$. The Nb_3Al sample was given a high-temperature homogenizing anneal for 10 h at 1700 °C plus a one-week ordering anneal at 750 °C. A small amount of σ phase, which usually occurs in high- T_c Nb_3Al , was detected in this sample.³⁷ Finally, the Nb_3Pt was also arc melted starting with spectroscopically pure Johnson Matthey Nb and 99.99%-pure Pt from Engelhard. The composition of the Nb_3Pt was nominally $Nb_{75.0}Pt_{25.0}$. The Nb_3Pt resistivity samples were cut from an ingot that was given a high-temperature homogenizing anneal at 180 °C for 12 h. After this cutting the specimens were given a low-temperature ordering anneal at 900 °C for ~ 3 weeks.

B. Neutron irradiation

The neutron irradiations were all carried out in the high flux beam reactor (HFBR) at Brookhaven National Laboratory. The HFBR uses ^{235}U as a fuel and is moderated and cooled with D_2O . The flux in the irradiation chamber is composed of a broad spectrum of neutron energies and can be broken down as follows: 1.3×10^{14} n/cm²sec for $E > 1$ MeV; 5.3×10^{14} n/cm²sec for $E > 0.1$ MeV; 1.9×10^{14} n/cm²sec for $E < 0.63$ eV; and a total flux of 12.1×10^{14} n/cm²sec. We have calculated our fluences on the basis of neutrons with $E > 1$ meV (i.e., using a flux

of $\sim 1.3 \times 10^{14}$ n/cm²sec). The determination of the flux was made by Argonne National Laboratory from a self-consistent computer fit to activation analysis data on 15 different pure metal foils irradiated in the HFBR.³⁸

The handling of the samples during irradiation has been described in detail elsewhere.³⁹ Briefly, for the first three irradiations of the single-crystal V₃Si, the sample was placed in a quartz tube sealed off in 0.5 atm of helium gas with the quartz tube fit tightly into a water-cooled aluminum capsule. For all other irradiations, the samples were wrapped in aluminum foil and packed tightly in fine mesh aluminum powder directly in the water-cooled aluminum capsule. It is estimated that the samples remained ≤ 200 °C throughout the irradiation.³⁹

C. Resistivity measurement

The resistivity ρ was measured as a function of temperature from T_c to room temperature. A standard four-probe technique was employed using an ac excitation current in the range of 10 mA at a frequency of ~ 15 Hz.⁴⁰ The absolute values of ρ at room temperature were obtained using knife-edge or point-voltage contacts with separations on the order of 1–2 mm. The overall reproducibility of this absolute measurement was $\sim 5\%$. The temperature dependence was measured either with the knife-edge contacts (first three irradiations of the V₃Si single crystal) or indium contacts (for all other irradiations) and the latter required normalization of the data to the room-temperature values. The two techniques gave temperature dependences within 1% of each other. The temperature scale was a calibrated germanium thermometer from 4.2 to 40 K and a calibrated platinum thermometer from 40 to 350 K. Thermal equilibrium was assured by thermally anchoring the sample and thermometers to a large copper block and making the measurement in helium exchange gas. The exchange gas chamber was surrounded by a uniformly bifilar wound heater extending well beyond the sample and thermometers and was further surrounded by a vacuum can. Finally, this outer vacuum can was immersed in liquid nitrogen or helium for cooling. Temperatures from ~ 2 to 4.2 K were obtained by pumping on liquid helium. Typically, two samples were mounted during one run and one was measured while cooling and the other while heating. The maximum heating or cooling rate was 1 K/min. Although the precision of the measuring instruments was ~ 0.1 to 0.2%, the overall reproducibility of the temperature dependences was on the order of 0.5%. Finally, the data acquisition was automated and the data were stored on tape to facilitate analysis.

III. PRESENTATION OF RESULTS

A. ρ -vs- T data

The ρ -vs- T data for the V₃Si single crystal for various irradiations (indicated in Table I) are presented in Fig. 1 (note that some of the irradiations have been omitted to avoid overcrowding). The polycrystalline V₃Si data (all samples from the same ingot) the Nb₃Pt, and the Nb₃Al data are all very similar to the single-crystal data and are not shown. The geometry of two of the Nb₃Al samples was so poorly suited for absolute ρ determinations that the absolute values were no better than 50%. In these cases, ρ was normalized by interpolation from a $\rho(295)$ versus fluence plot for the two good points. The most unifying feature of these data is the universal increase in ρ_0 with fluence and consequent reduction of the temperature-dependent contribution to the point where the slope of ρ vs T becomes flat and even negative. These results compare well in general with previous radiation studies on A15 compounds.^{6, 17–21}

B. RRR and $\rho(19)$ vs T_c

We have chosen T_c as a measure of damage for our irradiations rather than fluence (however, the fluence ϕt does appear in Table I) for several reasons. (i) The energy spectrum is not the same in all reactors and this makes difficult a comparison which is already hampered by the fact that there is no standard set of neutron energies defining fluence. Comparison to fluences for other types of irradiation

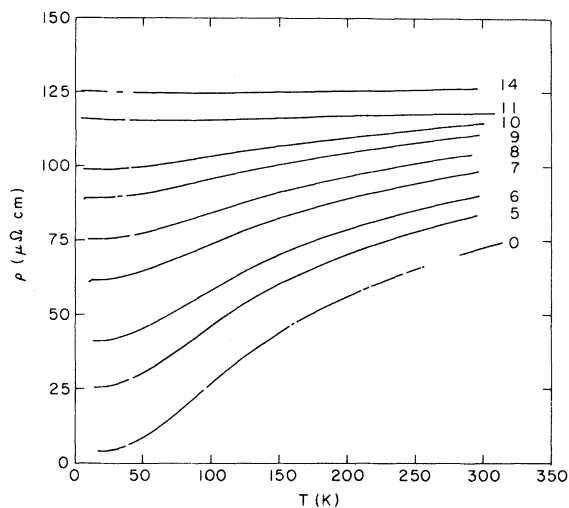


FIG. 1. ρ vs T for single-crystal V₃Si. The numbers after the curves refer to the irradiations listed in Table I.

TABLE I. The quantities T_c , RRR, $\rho(19)$, and ρ_0 (extrapolated as $\rho(T) = \rho_0 + bT^n$ from data in the temperature range 17 to 25 K) for the samples listed after neutron irradiation. *S* stands for single-crystal V_3Si ; *P1*, *P2*, and *P3* are three polycrystalline V_3Si samples from the same melt; *Pt1*, *Pt2*, and *Pt3* are three polycrystalline Nb_3Pt samples; and *A11*, *A12*, and *A13* are three polycrystalline Nb_3Al samples from the same melt. The number after the dash in the sample designation is the number of the neutron irradiation for that sample. The fluences are accurate to $\pm 1\%$; T_c 's to ± 0.1 K, RRR's to $\pm 0.5\%$; and $\rho(19)$'s and ρ_0 's to $\pm 5\%$.

Sample	Fluence (10^{18} n/cm 2)	T_c (K)	RRR	$\rho(19)$ ($\mu\Omega$ cm)	ρ_0 ($\mu\Omega$ cm)
S-0	0	16.90	16.6	4.22	3.78
S-1	0.25	16.65	18.3	3.84	3.41
S-2	1.65	16.60	16.2	4.32	3.86
S-3	3.53	16.70	18.8	3.74	3.23
S-4	5.40	15.95	7.48	9.35	8.79
S-5	8.21	13.95	3.23	25.9	25.2
S-6	11.0	12.27	2.18	41.4	40.8
S-7	14.5	10.25	1.588	61.8	61.4
S-8	18.0	8.97	1.383	75.5	75.5
S-9	21.5	6.96	1.237	89.4	89.3
S-10	25.0	5.69	1.154	99.1	99.1
S-11	28.5	4.83	1.108	106.7	106.6
S-12	36.0	3.71	1.061	113.9	113.9
S-13	43.5	2.78	1.030	121.3	121.0
S-14	88.4	2.44	1.011	125.2	124.6
P1-0	0	16.98	20.25	3.39	2.41
P1-1	0.23	16.98	13.6	5.01	...
P1-2	0.94	16.3	7.17	9.85	9.33
P1-3	2.57	15.23	4.00	18.1	17.5
P1-4	12.4	11.36	1.565	56.1	55.7
P1-5	46.1	3.7	1.018	115.8	115.0
P1-6	82.1	2.20	1.038	119.1	118.9
P1-7	127.0	<2.7	1.007	118.1	117.6
P2-1	0.7	16.36	7.79	9.3	...
P2-2	3.04	14.40	3.20	24.3	23.9
P2-3	6.55	11.86	1.985	42.0	41.4
P2-4	10.1	9.40	1.445	64.8	...
P2-5	13.6	8.24	1.282	78.0	...
P3-0	0	16.96	20.0	3.25	...
P3-1	1.64	15.83	5.47	12.7	...
P3-2	9.13	10.51	1.550	54.5	54.2
P3-3	12.6	8.40	1.311	70.3	70.2
P3-4	16.1	6.52	1.204	81.5	81.5
P3-5	41.8	2.58	1.024	113.4	113.4
Pt1-0	0	11.11	3.687	23.3	21.4
Pt1-1	7.5	6.45	1.105	87.0	87.0
Pt2-1	15.0	4.31	1.044	102.7	102.6
Pt3-1	202	3.03	1.013	110.6	...
A11-0	0	18.5	1.845
A11-1	7.5	12.88	1.204
A12-1	15.0	8.43	1.113
A13-1	202	3.71	0.997

is even more difficult. (ii) It is most likely that the irradiated samples are inhomogeneous on the scale of 40 Å and different starting samples behave very differently as a function of fluence.³⁹ (iii) We cannot completely discard the possibility that some annealing takes place during irradiation—especially for the longer irradiations. This would render fluence a doubtful measure of damage. Since T_c is very sensitive to damage, it is a good candidate for a measure of damage; however, one point should be made before using T_c as a measure of damage. The T_c we report is from resistivity measurements and does not necessarily represent the bulk T_c which would lie somewhat lower. We have reported⁴¹ T_c measurements from both resistivity and heat capacity on V_3Si as a function of neutron irradiation and find that, indeed, T_c of the bulk does lie lower than the resistively measured T_c . But this deviation is systematic as the sample is damaged and thus the resistive T_c , although it is not the bulk T_c , is a good measure of the damage.

In Fig. 2 we plot the residual resistivity ratio (RRR) versus T_c for all the data. We take the RRR to be defined as $\rho(295)/\rho(19)$. This behavior has been noted previously for nonoptimally deposited and α -damaged V_3Si films by Testardi *et al.*¹⁸ and their range of observed values is shown by the dashed lines in Fig. 5. Our values for neutron-damaged single and polycrystal V_3Si bulk samples agree well with the Testardi *et al.* data on V_3Si films. Note that the Nb_3Pt data for unirradiated samples lie well below the V_3Si curve and the Nb_3Al data for low doses lie well above. This most likely reflects the fact that the Nb_3Pt system produces the best quality metallurgical

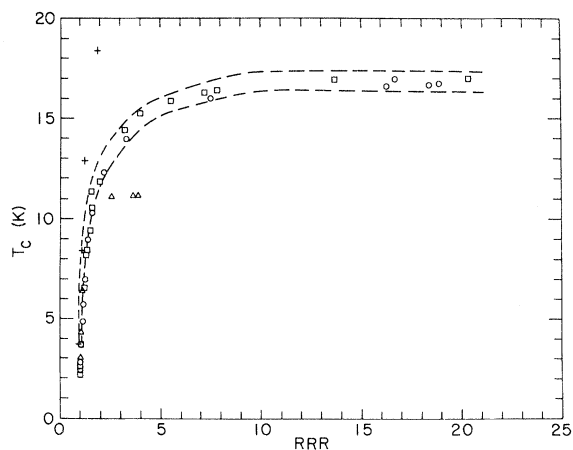


FIG. 2. T_c vs RRR for neutron-irradiated A15 compounds. \circ , single-crystal V_3Si ; \square , polycrystalline V_3Si ; Δ , polycrystalline Nb_3Pt ; $+$, polycrystalline Nb_3Al (the dashed line is from Ref. 18).

samples^{37,42} (closer to stoichiometry and less second phase) while the Nb_3Al system produces the worst,³⁷ with V_3Si in between.

$\rho(19)$ vs T_c is plotted in Fig. 3 and ρ_0 extrapolated from $\rho = \rho_0 + bT^n$ in the temperature range 17–25 K appears in Table I. For V_3Si the value of n is within ± 0.5 of 2.0 when there is appreciable temperature dependence. Larger values of n up to 4.6 are obtained for the more heavily damaged samples, but the values of ρ_0 obtained are within 1% (considerably less than the error in ρ_0) of those obtained by setting $n = 2$. For Nb_3Pt the values of n range from 2.7 to 4. Of course, $\rho(19)$ and ρ_0 differ, but the behavior with fluence is very similar. In the absence of any guiding principle, namely that we do not know if ρ_0 is a valid extrapolation, we chose $\rho(19)$ as a measure of the residual resistivity. The single and polycrystal V_3Si samples again behave in a very similar manner (except for initial damage region which is too compressed here—see Ref. 39) and all the data including Nb_3Pt and Nb_3Al coalesce at high $\rho(19)$ (similar to all the RRR's approaching unity). This is expected because most A15's saturate at approximately the same T_c (~ 2 –3 K) and ρ_{max} (~ 130 –140 $\mu\Omega$ cm). It should be noted here that our results in Fig. 3 agree well with those of Karkin *et al.*²¹ but we have not plotted the Russian results as the figure is already overcrowded.

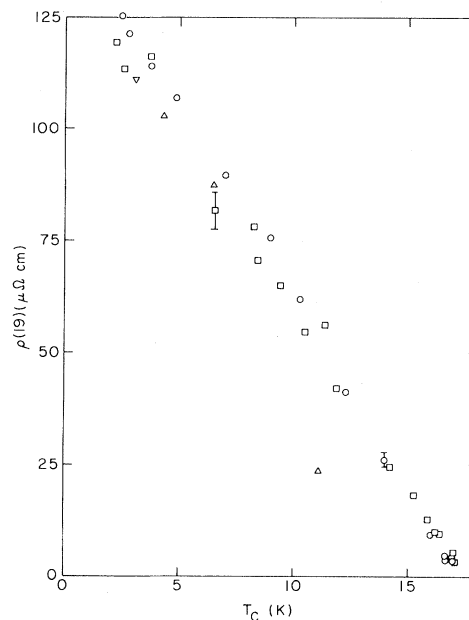


FIG. 3. $\rho(19)$ vs T_c for neutron-irradiated A15 compounds. $\rho(19)$ is the resistivity at 19 K. \circ , single-crystal V_3Si ; \square , polycrystalline V_3Si ; Δ , polycrystalline Nb_3Pt ; ∇ , polycrystalline Nb_3Al .

C. Data analysis

Each run from T_c to room temperature typically consisted of approximately 600 data points (ρ and T) which were initially stored on cassette tape and ultimately on magnetic tape accessible by the large Control Data 7600 computer at Brookhaven National Laboratory. Some of the analysis was done with the small HP9830 used to acquire the data, but most of the curve fitting was done on the large computer using a program developed at CERN called MINUIT.⁴³ With this program, it is possible to fit a curve to any function that can be written in closed form using an arbitrary number of parameters which are allowed to float. It achieves this by minimizing the square of χ (the deviation of the measured value from the fit curve). The minimization is accomplished by successively approximating the gradient of χ^2 in the multidimensional parameter space until at some particular set of parameters χ^2 is a minimum within specified tolerances. This powerful technique allows a fit to functions with exponential or logarithmic terms or even terms involving integrals where the limits contain the fit parameter and the variable such as the Bloch-Grüneisen function discussed in the Introduction.

D. Examples of fits and the fit parameters for the various theories

One should always check a fit by plotting it along with the data. In Figs. 4–6 we show the fits over the full temperature range for Eqs. (1), (3) with (4), or (3) with (5), respectively, for the same run on

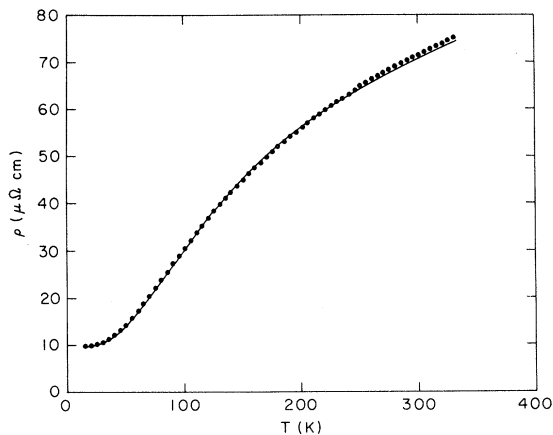


FIG. 4. Fit to $\rho = \rho_0 + \rho_1 T + C e^{-T_0/T}$ [Eq. (1)] for sample S-4 V_3Si of Table I. The solid line represents the data (actually many closely spaced data points) and the solid circles are the fit to the data.

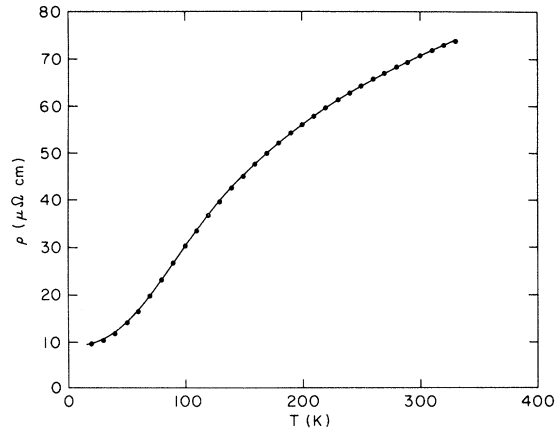


FIG. 5. Fit to the parallel resistor model with $\rho_{ideal} = \rho_{0l} + \rho_{sd}$ [Eqs. (3) and (4)] for sample S-4 V_3Si of Table I. The solid line represents the data (actually many closely spaced data points) and the solid circles are the fit to the data.

single-crystal V_3Si (irradiation 4). This run was representative of all the runs. Inspecting these quickly we see that all three fit the data reasonably well. However, there are stronger systematic deviations observable in the fits using Eqs. (1) and (3) with (5). In this comparison, and generally in the other runs, the parallel resistor model [Eq. (3)] with the ideal part of the resistivity described by Wilson's s - d scattering [see Eq. (4)] fits the data best. It should be cautioned that there are several parameters in these expressions and the good fits could be fortuitous. Figure 7 shows the fit to Eq. 7 over the more

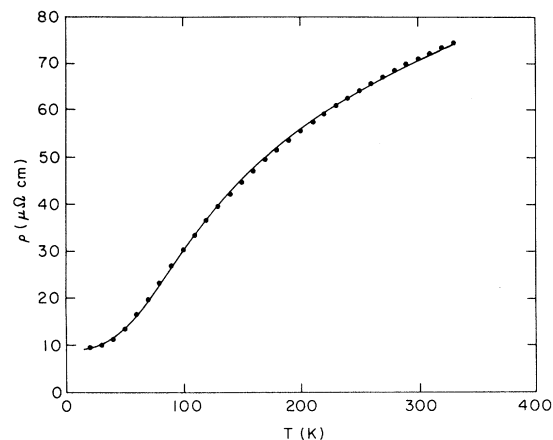


FIG. 6. Fit to the parallel resistor model with $\rho_{ideal} = \rho_{0l} + \rho_{Grün}$. [Eqs. (3) and (5)] for sample S-4 V_3Si of Table I. The solid line represents the data (actually many closely spaced data points) and the solid circles are the fit to the data.

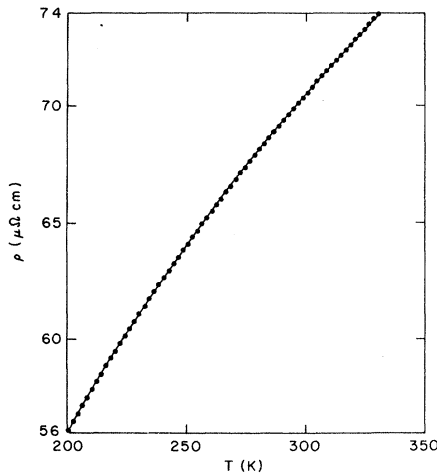


FIG. 7. Fit to $\rho = \rho_0 + A \ln(T/B)$ [Eq. (7)] for the sample S-4 V_3Si of Table I. The solid curve represents the data (actually many closely spaced data points) and the solid circles are the fit to the data.

limited temperature region of 200 K to room temperature since Gor'kov's theory is really only correct at high temperatures. Again, we use the data for the fourth irradiation of the single-crystal V_3Si . We defined the lower cutoff in temperature as 200 K because the logarithmic term cannot be fit through the inflection in the data at ~ 200 K. The fit is excellent but then we are considering only a limited temperature region.

Before presenting the fit parameters, we list a few important parameters [fluence, T_c , RRR, $\rho(19)$ and ρ_0] in Table I for all the samples and their irradiations. As a measure of the quality of the fit, the deviation given as a percentage of the fit from the measured data is defined as $100 \times [(\sum_{i=1}^N \chi_i^2)/N]^{1/2}$, where N is the number of data points in the fit region and $\chi_i = [\rho_i(T)_{\text{fit}} - \rho_i(T)_{\text{meas.}}]/\rho_i(T)_{\text{meas.}}$.

IV. DISCUSSION OF RESULTS

A. Results on V_3Si before irradiation

As there are many explanations put forth for the resistivity in $A15$ compounds, it would be best to discuss the results before irradiation first and this will naturally lead to the discussion of the neutron-irradiation results. For this discussion, we will only refer to the data on the single-crystal V_3Si as being representative of V_3Si . Before irradiation we obtained $\rho_1 = 0.029 \mu\Omega \text{ cm/K}$, $C = 108 \mu\Omega \text{ cm}$, and $T_0 = 170$ K from the fit to Eq. (1) over the temperature range T_c to 300 K. The deviation of the fit was 1.6%. [We fit to Eq. (1) because we were using

higher temperature data than appropriate for Eq. (2). Also ρ_0 was fixed to the extrapolated value in Table I.] Williamson and Milewits⁴ (WM) report values of $\rho_1 = 0.022 \mu\Omega \text{ cm}$, $C = 120 \mu\Omega \text{ cm}$, and $T_0 = 187$ K from analysis of Marchenko's²⁹ data taken from T_c to 1200 K on a polycrystalline V_3Si sample with RRR = 26. These values are in reasonable agreement with our results when one considers the following points. (1) The magnitude of the $\rho_1 T$ term in Eq. (1) is on the order of 10% throughout the whole temperature range and thus the fit is not too sensitive to the value ρ_1 and it is not surprising that the two values of ρ_1 are not in better agreement. (2) WM show that C and T_0 increase with RRR and the values from Marchenko's data are greater in accordance with his higher RRR (ours was only 17). (3) Fits in various temperature ranges show that inclusion of higher temperature data results in higher values of C and T_0 which is another source of the difference in the two sets of values. WM make the point that the contribution resulting in an exponential behavior below T_0 [see Eq. (1)] should become linear above T_0 . However, for the fit the exponential term becomes dominant at room temperature ranging from less than 1% of the total contribution to ρ at 20 K to around 80% from 150 to 300 K. The fit of the data above T_0 to a dominantly exponential term, according to the ideas expressed by WM, should be fortuitous.

As a check on the accuracy of T_0 (the physically meaningful parameter in their interpretation of the exponential term) WM vary T_0 by 30% and find that the deviation in the fit worsens from 1% to 4% for Nb_3Sn data in the temperature range T_c to 100 K. They conclude that T_0 (95 K for Nb_3Sn) is known to 10%. We carried out a similar analysis for our V_3Si data. For the data from T_c to 350 K we find that varying T_0 by 30% using Eq. (1) worsens the deviation from 1.5% to 10%. Following the same procedure just for the data from T_c to 50 K shows a change of only 0.2% to 0.6%. Thus, the fit is *least* sensitive to T_0 in the region where the exponential term is physically meaningful. If we use Eq. (2) to fit the data and allow the parameters ρ_0 , ρ_1 , n , and C to range freely while fixing T_0 and using data from T_c to 50 K, we find (see Table II) it hard to choose a value of T_0 since all fits are about equally good. Lastly, examination of Fig. 4 shows deviations in the fit curve outside the stated precision of 0.5%. All of these facts taken together lead us to conclude that the fit to Eq. (1) is indeed fortuitous and analysis of the irradiated samples further substantiates this claim as discussed below.

From Figs. 5 and 6 one can see that the parallel resistor model [Eq. (3)] fits the data much better if the Wilson s - d model is used for $\rho_l(T)$ rather than the Bloch-Grüneisen expression. In fact, Eqs. (3) and (4) fit the data better than the 0.5% uncertainty

TABLE II. Fit parameters for Eq. (2) for sample S-0 using data from the temperature range T_c to 50 K. (FIX) appearing after T_0 values indicates that T_0 was fixed to this value while the other parameters were still allowed to vary freely. ρ_1 was constrained < 0.02 and the entry > 0.02 (L) indicates the fit parameter was at this limit.

ρ_0 ($\mu\Omega$ cm)	ρ_1 ($\mu\Omega$ cm/K n)	n	C ($\mu\Omega$ cm)	T_0 (K)	Deviation (%)
3.80	0.0016	1.97	113	222	0.15
3.54	> 0.02 (L)	1.25	83	175(FIX)	0.22
3.69	0.005 14	1.64	103	200(FIX)	0.16
3.81	0.001 42	2.01	115	225(FIX)	0.15
3.86	0.000 737	2.19	136	250(FIX)	0.16
3.88	0.000 50	2.30	173	275(FIX)	0.16
3.90	0.000 396	2.37	231	300(FIX)	0.17

in the temperature dependence. The effect of varying the fit parameters $\rho_{\max}(sd)$ and Θ_{sd} is shown in Table III. The fit is much more sensitive to ρ_{\max} than to Θ_{sd} which may indicate that while the parallel resistor idea describes the data well the best form for $\rho_l(T)$ has not been determined. The cutoff temperature $\Theta_{sd} = 442$ K for sample S-0 is a reasonable value since this is close to the Debye temperature $\Theta_D \approx 410$ K reported for the same material.³⁴ Also, the value of $\rho_{\max}(sd) = 134 \mu\Omega$ cm is comparable to values reported for other $A15$ compounds (i.e., $\rho_{\max} \approx 135 \mu\Omega$ cm for Nb_3Ge ⁶). We did not try to fit to Eq. (6) but the better fit for $r = 3$ as opposed to $R = 5$ is in accord with the values $r = 2$ for Nb_3Sn and V_3Ge and $r = 3$ for Nb_3Sb obtained by Morton *et al.*⁷ It is worthwhile to point out that we also get a good fit to higher temperature data ($T \geq 200$ K) using $\rho_l(T) = LT$ and the values have been reported elsewhere.⁴⁴ We obtain a value of $L = 0.6 \pm 0.2 \mu\Omega$ cm/K with a deviation of 0.01% for sample S-0. This value of L is comparable to the $0.5 \mu\Omega$ cm/K

value obtained for Nb_3Ge ⁶. However, we require negative values of ρ_{0l} which may be a result of the low ρ_0 of V_3Si compared to Nb_3Ge .

Equation (7) describes the data in the temperature range 200 to 350 K extremely well as can be seen by reference to Fig. 7; in fact, the deviation is 0.13%. We obtain a value of $40 \mu\Omega$ cm for A and 55 K for B . Varying A and B for sample S-0 by 30% changes the deviation from 0.13% to 2.9% and 2.0%, respectively, so the fit is quite sensitive to these parameters. Testardi *et al.*¹⁸ report values for A and B of 49 $\mu\Omega$ cm and 55 K, respectively, for an optimally deposited V_3Si film with a T_c from 16.1 to 16.7 K. Our value of B is in excellent agreement and the difference in A could easily be due to the uncertainty in the absolute value of ρ .

The data for sample S-0 from 18 to 38 K are described well by $\rho = \rho_0 + bT^2$. This has been observed before for V_3Si by Marchenko²⁹ who reports $b = 0.007 \mu\Omega$ cm/K² for a sample with RRR = 26 and Milewits *et al.*²³ who report $b = 0.0016 \mu\Omega$ cm/K² for

TABLE III. Fit parameters for Eqs. (3) and (4) for sample S-0 using data from 200 to 350 K. (FIX) appearing after a parameter indicates that the parameter was fixed at the value listed while the other parameters were still freely varied. The parameters ρ_{0l} and κ_{sd} were constrained and the (L) after an entry indicates the parameters were at the set limits.

$\rho_{\max}(sd)$ ($\mu\Omega$ cm)	ρ_{0l} ($\mu\Omega$ cm)	Θ_{sd} (K)	κ_{sd} ($\mu\Omega$ cm)	Deviation (%)
143	4.9	396	407	0.06
100(FIX)	0(L)	543	1000(L)	2.6
186(FIX)	6.0	0.035	0.027	0.32
152	0(L)	250(FIX)	239	0.12
130	10(L)	560(FIX)	668	0.15

a sample with $RRR = 14$. Our value for $S-0$ with $RRR = 18$ is $b = 0.0015 \mu\Omega \text{ cm}/\text{K}^2$. All these values are in reasonable agreement. We also fitted to $\rho = \rho_0 + bT^n$ using data from 17 to 25 K for sample $S-0$ and obtained a value of $n = 1.94$ but the sensitivity of the fit to n was not very great. Using a program developed by Gurvitch⁴⁵ to plot deviations from a fit using various powers of n we determined n to be 2 ± 0.25 .

The suggestion of Webb *et al.*¹² that the low-temperature resistivity can be described by phonon-assisted $s-d$ interband scattering if one uses the real phonon density of states bears further scrutiny. Bader *et al.*⁵ fitted the V_3Si resistivity data of Milewits *et al.*²³ from T_c to 50 K using the phonon density of states obtained from neutron studies by Schweiss *et al.*⁴⁶ We followed the procedure described by Bader *et al.*⁵ to fit our data using the same phonon spectrum. Since this calculation only gives the temperature dependence and not the magnitude of the resistivity change, it is necessary to fix the scale of ρ at two temperatures (we chose 18 and 50 K). Thus it is very important to examine the fit carefully between the two temperatures where the fit resistivity and measured resistivity are constrained to be equal. In Fig. 8 we plot the deviation of the fit from the measured values between 18 and 50 K. Since we observed a systematic deviation, we then determined that the phonon spectrum calculation results in a T^3 rather than T^2 dependence in the resistivity. Two comments concerning the calculation are in order. First, the phonon spectrum data are difficult to obtain below 8 MeV and as this part of the spectrum makes a reasonable contribution to the low-temperature resistivity the method of extrapolating the data to zero energy could be important. We extrapolated the data as suggested by Schweiss *et al.*,⁴⁷ as ω^2 assuming a Debye spectrum at low ω , and finally using the model density of states calculated by Testardi and Mattheiss⁴⁸ from acoustic data. All three extrapolations gave an exponent of 3 ± 0.25 for the temperature dependence of resistivity. The second point is that we used the phonon spectrum at 4.2 K for the above calculation rather than a temperature-dependent spectrum. However, the temperature dependence of the phonon spectrum is not too large and we can check the effect of temperature dependence by using the phonon spectrum at 77 K and comparing. The resulting exponent is 3.25. Therefore, we can say with reasonable confidence that the resistivity calculated assuming phonon-assisted $s-d$ interband scattering using the actual phonon spectrum for V_3Si results more nearly in a T^3 dependence rather than the T^2 dependence observed by several investigators for high- T_c $A15$ superconductors. Although the T^2 and T^3 dependencies may be accidental, there is a definite discrepancy between calculation and experiment.

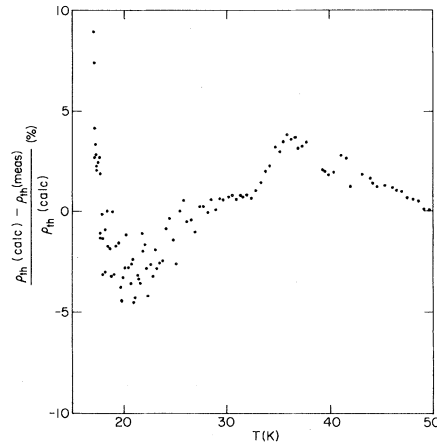


FIG. 8. $[\rho_{\text{th}}(\text{calc}) - \rho_{\text{th}}(\text{meas})]/\rho_{\text{th}}(\text{calc})$ vs T for sample $S-0$ of Table I. $\rho_{\text{th}}(\text{calc})$ is the calculated temperature-dependent contribution to the resistivity using the Karlsruhe phonon spectrum for V_3Si at 4.2 K. $\rho_{\text{th}}(\text{meas.})$ is the measured temperature-dependent contribution. Note $\rho_{\text{th}}(\text{calc})$ is constrained to equal $\rho_{\text{th}}(\text{meas.})$ at 18 and 50 K.

B. Results on V_3Si after irradiation

As mentioned in the Introduction, Meisel *et al.*²⁷ computed a normalized plot of T_c vs ρ_0 which is in good agreement with Nb_3Sn results. However, this agreement does not hold for V_3Si because their curve predicts a constant T_c for $\rho_0 \leq 40 \mu\Omega \text{ cm}$ and it would not be possible to fit our data in Fig. 3 onto this curve. T_c clearly continues to increase below the critical value of $\rho_0 \approx 40 \mu\Omega \text{ cm}$. It is possible that this difference could be due to the parameters used to generate their curve. The phonon spectrum for V_3Si is known to be considerably stiffer than that for Nb_3Sn and since the phonon spectrum is crucial to their calculation this difference could be the source of the different T_c vs ρ_0 behaviors of V_3Si and Nb_3Sn .

To present the neutron irradiation results for the fit to Eq. (1), we plot T_0/T_{00} vs T_c/T_{c0} in Fig. 9, where T_{00} and T_{c0} are the values for the unirradiated samples. We chose this normalized plot to make comparisons with other $A15$ compounds later in the paper and do not plot against fluence for reasons discussed in Sec. III B. We will concentrate on T_0 in this discussion; however, the following comments can be made about the other parameters. ρ_1 drops with neutron dose which reflects the diminishing magnitude of the thermal contribution to ρ . Similarly the parameter C drops for the same reason and also to partially compensate for the rise in T_0 . The data plotted in Fig. 9 for the single-crystal V_3Si and the three polycrystalline V_3Si samples all follow the same curve within the scatter of the fit parameter T_0 . In

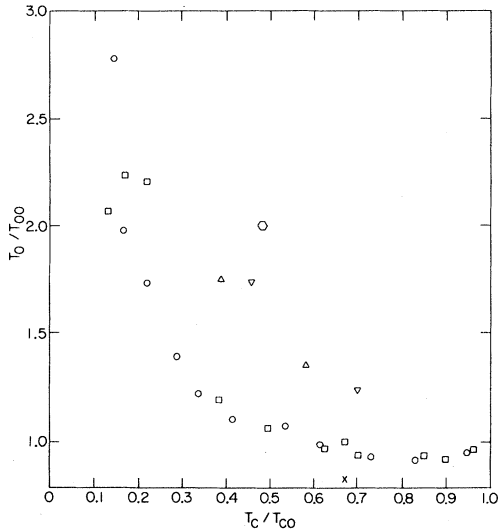


FIG. 9. T_0/T_{00} vs T_c/T_{c0} for A15 compounds. T_{00} and T_{c0} are the respective values of T_0 and T_c for the unirradiated samples. \circ , single-crystal V_3Si ; \square , polycrystalline V_3Si ; Δ , polycrystalline Nb_3Pt ; ∇ , polycrystalline Nb_3Al ; \times , V_3Si film (Ref. 18); \square , Nb_3Ge film (Ref. 18).

fact, a data point from Testardi *et al.*¹⁸ for a nonoptimally deposited V_3Si film is also in reasonable agreement with the bulk sample data and thus the results are quite similar irrespective of the form of the sample (i.e., single-crystal, polycrystal, or film). T_0 is relatively unaffected until a fractional reduction of T_c of approximately 0.5. At this point, T_0 begins to rise rather rapidly with further reduction in T_c by neutron damage. We will discuss this trend later in comparison with other A15 systems, but at present we just note that the ultimate increase in T_0 with reducing T_c is in agreement with the phenomenological observation of Fisk and Lawson¹ that T_c correlates with the location of the inflection point in the ρ vs T curve for high- T_c materials. They observe that the higher the inflection point ($T_0/2$), the lower the T_c . However, it should be pointed out that the rise in T_0 with damage is inconsistent with the proposals of Woodard and Cody²² or Milewits, Williamson, and Taub,²³ where T_0 represents the phonon energy necessary to scatter electrons between bands or different pockets of the Fermi surface. The damage should smear out the electronic band structure, thereby decreasing T_0 and not increase it as we observe.

Turning to the fits to the parallel resistor model, the values of $\rho_{\max}(sd)$ and $\rho_{\max}(R)$ do not seem to have any significant trend as a function of neutron damage and this result is in agreement with previous observations on other A15 compounds.^{6,19} The values of κ_{sd} and κ_R are too scattered to make any definite statements. The cutoff temperatures Θ_{sd} and

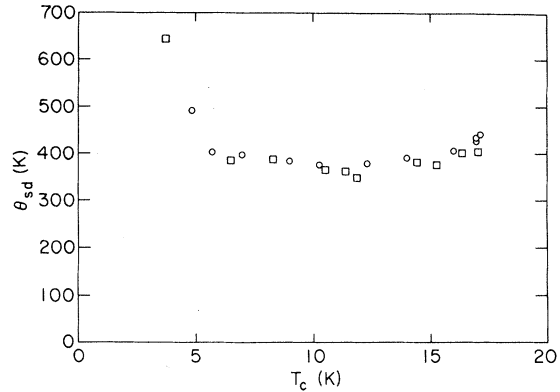


FIG. 10. Θ_{sd} vs T_c . \circ , single-crystal V_3Si ; \square , polycrystalline V_3Si .

Θ_R show less scatter probably because they measure the shape of the ρ vs T curve and do not depend on the poorly determined magnitude of ρ . In Figs. 10 and 11 we plot Θ_{sd} and Θ_R as a function of T_c . There is very little change in Θ_{sd} or Θ_R down to $T_c \sim 5$ K. The increase in Θ_{sd} and Θ_R seen below 5 K is in the direction observed from heat-capacity measurements³⁴ on neutron-irradiated V_3Si . It is possible that our observed increase is due to a breakdown of the fit as the thermal part of ρ becomes very small. The constancy of the cutoff temperature agrees with the analysis of Gurvitch *et al.*¹⁹ of their Mo_3Ge data where they find that one value of Θ_R fits all their ρ vs T curves for successively α -particle-damaged samples.

Similarly, as for the T_0 results we plot B/B_0 vs T_c/T_{c0} from the fit to Eq. (7) in Fig. 12; here B_0 is the value of B for the unirradiated samples. Again, the results for the single crystal V_3Si and three polycrystalline V_3Si samples agree nicely with each other

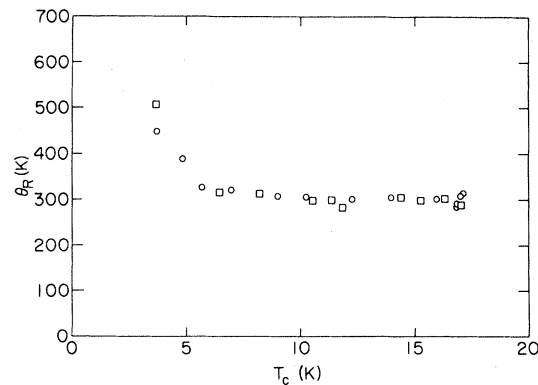


FIG. 11. Θ_R vs T_c . \circ , single-crystal V_3Si ; \square , polycrystalline V_3Si .

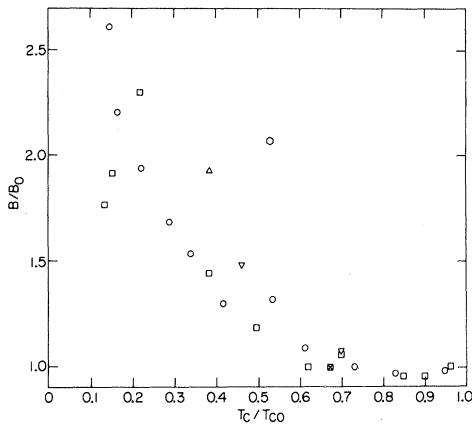


FIG. 12. B/B_0 vs T_c/T_{c0} . B_0 and T_{c0} are the respective values of B and T_c for the unirradiated samples. \circ , single-crystal V_3Si ; \square , polycrystalline V_3Si ; Δ , polycrystalline Nb_3Pt ; ∇ , polycrystalline Nb_3Al ; \times , V_3Si film (Ref. 18); \diamond , Nb_3Ge film (Ref. 18).

and a nonoptimally deposited V_3Si film.¹⁸ The same type of behavior in B/B_0 is seen as for T_0/T_{00} and this is most likely due to the fact that both parameters are sensitive to the shape of ρ vs T and not the magnitude of ρ . The parameter A is dependent on the magnitude of ρ and Testardi¹⁸ has noted a correlation of this parameter with T_c . In Fig. 13 we plot A vs T_c for all the V_3Si samples where the suggested linear dependence of A and T_c can be clearly seen.

The most striking feature of the V_3Si ρ vs T data (which has been mentioned elsewhere⁴⁴) is that while the magnitude of the thermal contribution to ρ drops with damage the shape remains essentially unchanged down to $T_c/T_{c0} \sim 0.5$. This feature is responsible for the behaviors of T_0 and B .

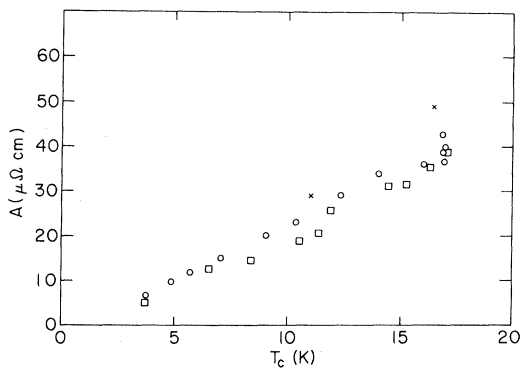


FIG. 13. A vs T_c . \circ , single-crystal V_3Si ; \square , polycrystalline V_3Si ; \times , V_3Si film (Ref. 18).

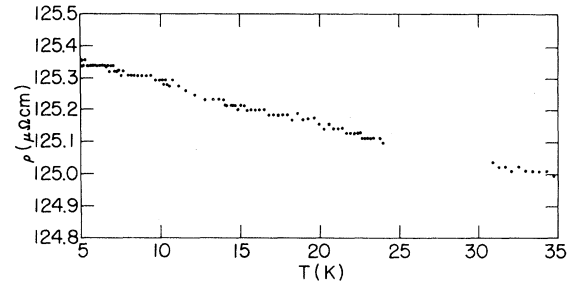


FIG. 14. ρ vs T for low-temperature data on sample S-14 of Table I.

The low-temperature resistivity of all the V_3Si samples follows a T^2 dependence for samples damaged to the point where T_c has dropped to ~ 6 K. For heavier damaged samples, we observe a linear dependence in ρ (with negative slope) vs T as plotted in Fig. 14 rather than the negative T^2 dependence predicted by Cote *et al.*⁸ The values of b from a fit to $\rho = \rho_0 + bT^2$ are shown in Fig. 15 as a function of T_c for those V_3Si samples which still followed a T^2 dependence at low T . On the same graph, we have plotted the square of the coefficient of the linear term in the specific heat γ from data on a single crystal of V_3Si which was adjacent to the resistivity sample in the master boule.³⁴ The correlation between b and γ^2 is striking, but as mentioned before the magnitude of b seems to be much too large (a factor of 16) for the electron-electron scattering mechanism noted in transition elements.

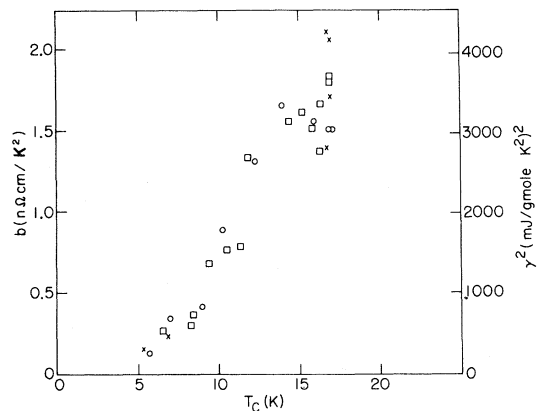


FIG. 15. b vs T_c and γ^2 vs T_c . \circ , single-crystal V_3Si data for b ; \square , polycrystalline V_3Si data for b ; \times , single-crystal V_3Si data for γ^2 (Ref. 34).

C. Results of other $A15$ compounds and comparison to V_3Si

Also appearing on Fig. 9 are our results for Nb_3Pt and Nb_3Al and the results of Testardi *et al.*¹⁸ for Nb_3Ge films damaged by α particles. The results for the Nb-based $A15$'s do not show the same trend as the V_3Si data. T_0 drops much more continuously with T_c for the Nb-based $A15$'s and does not show the striking constancy down to $T_c/T_{c0} \sim 0.5$ demonstrated by the V_3Si system. It has been shown that V_3Si does not disorder nearly as much as the Nb-based $A15$'s for a similar drop in T_c .³⁶ Perhaps T_0 is more sensitive to disorder than T_c and the quicker increase in T_0 for the Nb-based $A15$'s is related to the greater disorder in these systems. This conjecture is supported by two other facts. (1) Our observed value of T_0 for Nb_3Pt (78 K) is lower than that we observe for Nb_3Al (102 K) even though T_c is much higher for Nb_3Al which is consistent because Nb_3Pt is known to be inherently more ordered than Nb_3Al .^{16,41} The correlation seems to be the lower T_0 the greater the order (and of course T_c is related to the degree of order in the system). (2) In the Mo_3Ge system,¹⁹ T_c increases with greater disorder (as opposed to all other $A15$'s) but it appears as if T_0 is also increasing with disorder; so, again, the correlation is with order and not T_c . Thus it seems plausible that the inflection in ρ vs T at $T_0/2$ phenomenologically correlates with disorder rather than T_c and that the correlation with T_c results from the fact that more highly ordered superconductors usually have a greater T_c —all else being equal.

The unirradiated Nb_3Pt and Nb_3Al data also fit the parallel resistor model reasonably well with one notable difference. For Nb_3Pt the Wilson s - d model works best for $\rho_l(T)$ as in the V_3Si case, but for Nb_3Al the Bloch-Grüneisen expression characterizes $\rho_l(T)$ better. The values for $\rho_{\max}(sd) = 102 \mu\Omega \text{ cm}$ and $\rho_{\max}(R) = 105 \mu\Omega \text{ cm}$ for Nb_3Pt while lower than for V_3Si are still the right order of magnitude. Also, the cutoff temperatures $\Theta_{sd} = 274 \text{ K}$ and $\Theta_R = 210 \text{ K}$ for Nb_3Pt and $\Theta_{sd} = 203 \text{ K}$ and $\Theta_R = 170 \text{ K}$ for Nb_3Al are reasonable since Θ_D is known to be lower in Nb_3Pt (Ref. 49) and Nb_3Al (Ref. 48) than V_3Si (in agreement with our relative values). Unfortunately the fits could not be done on the irradiated Nb_3Pt or Nb_3Al samples.

Although it is not as clear as for T_0 , the parameter B does seem to drop more continuously for the Nb-based $A15$'s (see Fig. 12) probably for the same reason as T_0 drops more continuously. We could not get good enough absolute ρ values for Nb_3Al to warrant reporting values for A , but for the Nb_3Pt system we see the same linear correlation of A with T_c as observed for V_3Si .

The low-temperature behavior of the resistivity of Nb_3Pt is quite different from that of V_3Si while

Nb_3Al behaves similarly to V_3Si . The as-cast samples of Nb_3Pt exhibit a T^5 behavior at the lowest T (15–27 K) and a $T^{2.5}$ dependence for higher T (27–43 K). After the heat treatments previously described, the behavior changes to T^3 at the lowest T (12–27 K) and T^2 at higher T (24–43 K). It is as if the T^2 behavior has been shifted to higher temperatures compared to V_3Si . It is interesting to note that Mo_3Ge with a low T_c ($\sim 1.5 \text{ K}$) shows a T^5 dependence at low T . It appears as if the lower T_c materials have a higher power temperature dependence just above T_c . Further, the state of the material (as cast or heat treated), which is related to the degree of order, has a pronounced effect on the low- T temperature dependence. Nb_3Al ($T_c = 18.5 \text{ K}$), as previously reported,¹² shows a T^2 dependence from 20–43 K and in this respect is similar to V_3Si .

After the lowest-dose irradiation of the heat-treated Nb_3Pt (which lowered T_c from 11.1 to 6.5 K) the region of T^3 behavior moved up in temperature to 22–36 K and from 36–43 K the behavior was T^2 . This is consistent with a higher power of T dependence over a greater temperature range for lower T_c materials. The next dose (which lowered T_c to 4.3 K) produced a weaker temperature dependence which was very hard to characterize as anything but linear. The low-temperature data for the heaviest dose was not of sufficient quality to lend itself to analysis. For the Nb_3Al system, the first dose (which dropped T_c from 18.5 to 12.9 K) produced no effect on the low-temperature behavior. However, for the second dose (which dropped T_c to 8.4 K) the data fit a T^3 dependence better than a T^2 dependence from 20 to 43 K which is in accord with the Nb_3Pt observations. Finally, the heaviest dose produced a flat temperature dependence at low temperatures typical of the heavily damaged V_3Si samples.

V. CONCLUSION

We have studied the effect on the normal-state resistivity of systematically lowering the T_c of $A15$ superconductors through neutron damage. As noted previously for radiation damage in $A15$ compounds, ρ_0 increases and the temperature-dependent contribution decreases with damage. However, for V_3Si there is very little change of shape (as evidenced by the constancy of T_0 , B , Θ_{sd} , and Θ_R) in the temperature-dependent part of the resistivity down to a fractional reduction in T_c of ~ 0.5 . The Nb-based $A15$'s seem to show a steadier change in shape with reduction in T_c . This could be related to the different sensitivity of T_c to order in V_3Si as compared to Nb-based $A15$'s. A V_3Si sample with a fractional reduction in T_c of 0.5 is much more ordered than a Nb-based $A15$ with the same fractional reduction. Perhaps the degree of order of the sample is a more

sensitive indication of a change in shape of the temperature-dependent contribution to the resistivity than T_c is.

In comparing the fit to the data of the various theories, it appears that they all have enough parameters to give a good fit but the parallel resistor model with the s - d scattering model of Wilson for the ideal contribution seems to fit best over the entire temperature range and the parameters required are physically reasonable. Also the analysis of the data indicates that the fits to Eqs. (1) or (2) are most likely fortuitous. It is of interest to note that the fits for all theories continue to work down to quite large reductions in T_c .

The low-temperature data for the high- T_c $A15$'s V_3Si and Nb_3Al exhibit a T^2 dependence while the heat-treated Nb_3Pt ($T_c = 11.1$ K) exhibits a T^3 dependence at the lowest temperatures. Upon irradiation, V_3Si maintains a T^2 dependence down to a damage level where $T_c \sim 6$ K. At this point, it becomes harder to fit the data but the dependence is most likely linear. The T^2 dependence in Nb_3Al changes to a higher power ($\sim T^3$) when T_c has been lowered to 8.4 K. For Nb_3Pt the radiation damage initially extended the range of the T^3 behavior and for a heavier dose produced a weak linear dependence. Again, as was seen for the shape of the ρ vs T curves, the effects of radiation on the form of the low- T temperature dependence were more noticeable in the Nb-based alloys at lower doses and lower fractional T_c reductions.

It is clear that there is much to ponder regarding

the effect of radiation damage on the normal-state resistivity of $A15$ superconductors. Hopefully, this information will be useful when examining existing and new theories attempting to explain the behavior of the resistivity in the normal state of $A15$ compounds.

ACKNOWLEDGMENTS

It is a pleasure to acknowledge Bob Jones for his expert handling of the neutron irradiations for all samples discussed in this paper and Chuck Tierney for his technical assistance throughout the experiment. We thank L. Testardi for the V_3Si single crystal and S. Moelecke for his excellent Nb_3Al samples. One of us (R.C) wishes to thank his good friend Howard Gordon for his introduction to and patient guidance through MINUIT and also Marilyn McKeown for her able programming assistance. We thank S. D. Bader for sending us detailed phonon spectrum data on V_3Si from Karlsruhe. For many useful and helpful discussions we acknowledge C. L. Snead, C. S. Pande, M. Strongin, A. K. Ghosh, M. Gurvitch, S. D. Bader, and L. Testardi. We also thank D. O. Welch for this careful reading of the manuscript and useful critical comments. We would like to thank and acknowledge M. Suenaga, D. H. Gurinsky, and Myron Strongin for their support. Finally, this work was performed under the auspices of the U.S. Department of Energy under Contract No. DE-AC02-76CH00016.

*Present address: Physics Department, Clarkson College of Technology, Potsdam, N.Y. 13676.

- ¹Z. Fisk and A. C. Lawson, *Solid State Commun.* **13**, 277 (1973).
²H. Lutz, H. Weisman, M. Gurvitch, A. Goland, O. F. Kammerer, and M. Strongin, in *Superconductivity in d- and f-band Metals—Second Rochester Conference*, edited by D. H. Douglass (Plenum, New York, 1976), p. 535.
³Z. Fisk and G. W. Webb, in Ref. 2, p. 545.
⁴S. J. Williamson and M. Milewits, in Ref. 2, p. 551.
⁵S. D. Bader and F. Y. Fradin, in Ref. 2, p. 567.
⁶H. Wiesmann, M. Gurvitch, H. Lutz, A. Ghosh, B. Schwarz, M. Strongin, P. B. Allen, and J. W. Halley, *Phys. Rev. Lett.* **38**, 782 (1977).
⁷N. Morton, B. W. James, and G. H. Wostenholm, *Cryogenics* **18**, 131 (1978).
⁸P. J. Cote and L. V. Meisel, *Phys. Rev. Lett.* **40**, 1586 (1978).
⁹B. Chakraborty and P. B. Allen, *Phys. Rev. Lett.* **42**, 736 (1979).
¹⁰G. T. Meaden, *Electrical Resistivity of Metals* (Plenum, New York, 1965), p. 98.
¹¹M. P. Sarachik, G. E. Smith, and J. H. Wernick, *Can. J. Phys.* **41**, 1542 (1963).

- ¹²G. Webb, Z. Fisk, J. E. Englehardt, and S. D. Bader, *Phys. Rev. B* **15**, 2624 (1977).
¹³V. M. Pan, I. E. Bulakh, A. L. Kasatkin, and A. D. Shevchenko, *J. Less Common Met.* **62**, 157 (1968).
¹⁴J. A. Woollam and S. A. Alterovitz, *Phys. Rev. B* **19**, 749 (1979).
¹⁵Ref. 10, p. 51.
¹⁶A. R. Sweedler, D. E. Cox, and S. Moehlecke, *J. Nucl. Mater.* **72**, 50 (1978), and references therein.
¹⁷A. K. Ghosh, H. Weismann, M. Gurvitch, H. Lutz, O. F. Kammerer, C. L. Snead, A. Goland, and M. Strongin, *J. Nucl. Mater.* **72**, 70 (1978).
¹⁸L. R. Testardi, J. M. Poate, and H. J. Levinstein, *Phys. Rev. B* **15**, 2570 (1977).
¹⁹M. Gurvitch, A. K. Ghosh, B. L. Gyorffy, H. Lutz, O. F. Kammerer, J. S. Rosner, and M. Strongin, *Phys. Rev. Lett.* **41**, 1616 (1978).
²⁰A. E. Karkin, B. N. Goshchitskii, V. E. Arkhipov, E. E. Valieu and S. K. Sidorov, *Phys. Status Solidi A* **46**, K87 (1978).
²¹A. E. Karkin, V. E. Arkhipov, V. A. Marchenko, and B. N. Goshchitskii, *Phys. Status Solidi A* **53**, K53 (1979).
²²D. W. Woodard and G. D. Cody, *Phys. Rev.* **136**, A166 (1964).

- ²³M. Milewits, S. J. Williamson, and H. Taub, *Phys. Rev. B* **13**, 5199 (1976).
- ²⁴R. W. Cohen, G. D. Cody, and J. J. Halloran, *Phys. Rev. Lett.* **19**, 840 (1967).
- ²⁵P. B. Allen, W. E. Pickett, K. M. Ho, and M. L. Cohen, *Phys. Rev. Lett.* **40**, 1532 (1978).
- ²⁶J. M. Ziman, *Philos. Mag.* **6**, 1013 (1961).
- ²⁷L. V. Meisel and P. J. Cote, *Phys. Rev. B* **19**, 4514 (1979).
- ²⁸L. P. Gor'kov, *Sov. Phys. JETP* **38**, 830 (1974) [*Zh. Eksp. Teor. Fiz.* **65**, 1658 (1973)].
- ²⁹V. A. Marchenko, *Sov. Phys. Solid State* **15**, 1261 (1973) [*Fiz. Tverd. Tela* **15**, 1893 (1973)].
- ³⁰M. J. Rice, *Phys. Rev. Lett.* **20**, 1439 (1968).
- ³¹L. R. Testardi, J. M. Poate, W. Weber, W. M. Augustyniak, and J. H. Barrett, *Phys. Rev. Lett.* **39**, 716 (1977).
- ³²C. Pande, *Solid State Commun.* **24**, 241 (1977).
- ³³E. S. Greiner and H. Mason, Jr., *J. Appl. Phys.* **35**, 3058 (1964).
- ³⁴R. Viswanathan and R. Caton, *Phys. Rev. B* **18**, 15 (1978).
- ³⁵A. Guha, M. P. Sarachik, F. W. Smith, and L. R. Testardi, *Phys. Rev. B* **17**, 9 (1978).
- ³⁶D. E. Cox and J. A. Tarvin, *Phys. Rev. B* **17**, 22 (1978).
- ³⁷S. Moechlecke, Ph.D. thesis (University of Campinas, Brazil, 1977) (unpublished).
- ³⁸R. R. Heinrich (private communication).
- ³⁹R. Viswanathan, R. Caton, and C. S. Pande, *J. Low Temp. Phys.* **30**, 503 (1978).
- ⁴⁰The data for the V₃Si single crystal before irradiation were taken at ~200 Hz. Subsequent checks showed ρ to be frequency independent from ~5 to 200 Hz.
- ⁴¹R. Viswanathan, R. Caton, and C. S. Pande, *Phys. Rev. Lett.* **41**, 906 (1978).
- ⁴²S. Moelecke, D. E. Cox, and A. R. Sweedler, *Solid State Commun.* **23**, 703 (1977).
- ⁴³F. James, computer code MINUIT (CERN Program Library D506, Geneva, Switzerland, 1971).
- ⁴⁴R. Caton and R. Viswanathan, *J. Phys. (Paris)* **C6**, 385 (1978).
- ⁴⁵M. Gurvitch, Ph.D thesis (State University of New York at Stony Brook, 1978) (unpublished).
- ⁴⁶B. P. Scheiss, B. Renker, E. Schneider, and W. Reichardt, in Ref. 2, p. 189.
- ⁴⁷Private communication from S. Bader.
- ⁴⁸L. R. Testardi, in *Physical Acoustics*, edited by W. P. Mason and R. N. Thurston, (Academic, New York, 1973) Vol. 10, p. 261.
- ⁴⁹R. Flukiger, Ph.D. thesis (University of Geneva, 1972) (unpublished).